

Nonlinear processes upon doubling the period of self-modulation oscillations in a solid-state ring laser

I.I. Zolotoverkh, A.A. Kamyshev, N.V. Kravtsov, E.G. Lariontsev, V.V. Firsov, S.N. Chekina

Abstract. Nonlinear phenomena appearing in a solid-state ring laser upon approaching the period-doubling bifurcation point of self-modulation oscillations and inside the doubling region are studied theoretically and experimentally. The bifurcation appears due to the parametric interaction of self-modulation oscillations of the first kind with relaxation oscillations. It is found that the bifurcation diagrams, time dependences of the intensities and power spectrum can significantly differ for counterpropagating waves because of the amplitude nonreciprocity of the ring resonator and the inequality of the moduli of the feedback coefficients. It is shown that when the self-modulation period is doubled, the widths of spectral peaks corresponding the self-modulation frequency and the fundamental relaxation frequency decrease. Noise precursors of doubling bifurcation are studied. It is found that the distance between the peaks of noise precursors increases with increasing the noise intensity. It is demonstrated experimentally that the noise modulation leads to the bifurcation point displacement, which increases with increasing the noise.

Keywords: solid-state ring laser, parametric synchronisation, self-modulation lasing regime of the first kind, period doubling of the self-modulation oscillations, amplitude nonreciprocity.

1. Introduction

Solid-state ring lasers (SRLs) are known to have many different nonstationary lasing regimes. The nonstationary regimes are realised both in autonomous [1] and in non-autonomous ring lasers upon periodic modulation of their parameters [2]. One of the most widespread nonstationary regimes in an autonomous SRL is a self-modulation regime of the first kind, which is characterised by the out-of-phase sinusoidal intensity modulation of counterpropagating waves [1]. This regime involves two relaxation frequencies – fundamental (ω_r) and additional (ω_{r1}). If the self-modulation frequency ω_m approaches the doubled value of one of the relaxation frequencies, a number of nonlinear effects appear which are related to the parametric

interaction of self-modulation and relaxation oscillations. This interaction can result in the instability of the self-modulation lasing regime of the first kind and in the excitation of more complex self-modulation oscillations (including the dynamic chaos) [3–6]. During the parametric resonance with the fundamental relaxation frequency, the period-doubling bifurcation of self-modulation oscillations is observed as a rule.

The period-doubling bifurcation appears in dynamic systems of different types (see, for example, [7–10] and references therein). The sequence of such bifurcations is typical for the transition to the chaos according to the Feigenbaum scenario [10]. Nonlinear phenomena accompanying the period-doubling bifurcation were studied in many papers. The parametric amplification of weak modulating signals (as well as noises) was considered near the bifurcation point at resonance frequencies close to the half the fundamental frequency [7–9, 11, 12]. This amplification proves to be phase sensitive and under certain phase relations these signals (noises) are attenuated [13, 14], i.e. phenomena similar to the light compression in a parametric oscillator are observed. The noise precursors of the period-doubling bifurcation were studied in papers [15, 16] and it was shown in [17, 18] that at certain noise intensities optimal (resonance) excitation of precursors was observed.

The majority of the mentioned papers are related to single (isolated) dynamic systems, while the coupled systems have not been thoroughly studied so far. The effects caused by the influence of noises in the vicinity of the period-doubling bifurcation are also hardly investigated experimentally. A solid-state ring laser can be treated as a system of two coupled unidirectional lasers and the study of the processes proceeding in counterpropagating waves during the doubling bifurcation helps reveal the peculiarities caused by the coupling between dynamic systems and non-identity of the interacting systems.

The aim of this paper is to study theoretically and experimentally the phenomena taking place in a two-directional ring laser near the bifurcation point and inside the region of parametric synchronisation of self-modulation and relaxation oscillations. The effect of system intrinsic noises and additional pump noise is considered.

2. Theoretical model and laser parameters

We used the vector model of a solid-state ring laser in the theoretical analysis of the phenomena under study [1, 19]. In this model, the radiation polarisation of counterpropagating waves is assumed specified and is characterised by the arbitrary unit vector $e_{1,2}$ for counter-

I.I. Zolotoverkh, A.A. Kamyshev, N.V. Kravtsov, E.G. Lariontsev, V.V. Firsov, S.N. Chekina D.V. Skobel'tsyn Institute of Nuclear Physics, M.V. Lomonosov Moscow State University, Vorob'evy gory, 119992 Moscow, Russia; e-mail: e.lariontsev@yahoo.com

propagating directions. The initial system of equations of the vector model has the form:

$$\begin{aligned} \frac{d\tilde{E}_{1,2}}{dt} &= -\frac{\omega_c}{2Q_{1,2}}\tilde{E}_{1,2} \pm i\frac{\Omega}{2}\tilde{E}_{1,2} + \frac{i}{2}\tilde{m}_{1,2}\tilde{E}_{2,1} \\ &+ \frac{\sigma l}{2T}(N_0\tilde{E}_{1,2} + N_{\mp}\tilde{E}_{2,1}), \\ \frac{dN_0}{dt} &= \frac{1}{T_1}[N_{th}(1+\eta) - N_0 - N_0a(|E_1|^2 + |E_2|^2) \\ &- N_+aE_1E_2^* - N_-aE_1^*E_2] + g_w, \\ \frac{dN_{\pm}}{dt} &= -\frac{1}{T_1}[N_{\pm} + N_{\pm}a(|E_1|^2 + |E_2|^2) + \beta N_0aE_1^*E_2]. \end{aligned} \quad (1)$$

Here, $\tilde{E}_{1,2}(t) = E_{1,2}\exp(i\varphi_{1,2})$ are the complex field amplitudes of counterpropagating waves; N_0 , N_{\pm} are spatial harmonics of the inverse population N determined by the expressions

$$N_0 = \frac{1}{L}\int_0^L N dz, \quad N_{\pm} = \frac{1}{L}\int_0^L e_i^* e_2 N \exp(\pm i2kz) dz; \quad (2)$$

L is the perimeter of the ray contour. System of equations (1) differs from the equations of the standard model [1] by the presence of the polarisation factor in the latter

$$\beta = (\mathbf{e}_1 \mathbf{e}_2)^2 = \cos^2 \gamma, \quad (3)$$

where γ is the angle between unite vectors $\mathbf{e}_{1,2}$. Note that the field polarisations of counterpropagating waves inside the resonator as well as the angle between the vectors $\mathbf{e}_{1,2}$ depend on the coordinate of the considered point inside the resonator. Expression (3) involves the value γ averaged over the resonator length. Another distinctive feature of equations (1) is the presence of the Gaussian noise g_w describing the noise modulation of the pump and having the following statistical characteristics:

$$\langle g_w(t) \rangle = 0, \quad (4)$$

$$\langle g_w(t)g_w(s) \rangle = D\delta(t-s), \quad (5)$$

where D is the noise intensity; $\delta(t)$ is the Dirac delta function.

Equations (1) use the following notations: $\omega_c/Q_{1,2}$ are the resonator bandwidths; $Q_{1,2}$ are the resonator Q factors for counterpropagating waves; $T = L/c$ is the round-trip time of light in the resonator; T_1 is the time of the longitudinal relaxation; l is the active element length; $a = T_1 c \sigma / (8\pi \hbar \omega)$ is the saturation parameter; σ is the laser transition cross section; $\Omega = \omega_1 - \omega_2$ is the frequency nonreciprocity of the resonator; ω_1 , ω_2 are the resonator eigenfrequencies for counterpropagating waves. The pump rate is represented in the form $N_{th}(1+\eta)/T_1$, where N_{th} is the threshold inversion population; $\eta = P/P_{th} - 1$ is the pump power excess over the threshold. The linear coupling of counterpropagating waves is determined by phenomenologically introduced complex coupling coefficients

$$\tilde{m}_1 = m_1 \exp(i\vartheta_1), \quad \tilde{m}_2 = m_2 \exp(-i\vartheta_2), \quad (6)$$

where $m_{1,2}$ are the moduli of coupling coefficients and $\vartheta_{1,2}$ are their phases. Note that equations (1) are written for the case of lasing at the gain line centre.

In the numerical simulation a part of the parameters was assumed equal to the experimentally measured correspond-

ing parameters of the laser under study. The resonator bandwidth was determined by the relaxation frequency $\omega_r = [\eta\omega_c/(QT_1)]^{1/2}$. When the pump is exceeded over the threshold $\eta = 0.09$, the main relaxation frequency in the laser under study is $\omega_r/2\pi = 65$ kHz. The polarisation parameter $\beta = 0.75$ was determined as in [19] by the experimentally measured dependence of the additional relaxation frequency ω_{r1} on the frequency nonreciprocity Ω of the resonator. The amplitude nonreciprocity of the ring resonator $\Delta = \omega_c/Q_2 - \omega_c/Q_1$ was determined by the experimentally measured phase difference of signals of self-modulation intensities of counterpropagating waves (see [1]). The values of the moduli and the phase difference of complex coupling coefficients $\tilde{m}_{1,2}$ are difficult to estimate by the characteristics of self-modulation oscillations. The results of the numerical simulation performed in this paper showed that the parameters of the self-modulation oscillations in the bifurcation region of their period doubling are most strongly affected by the frequencies ω_m and ω_r , the inequality of the moduli of the coupling coefficients $m_{1,2}$ and the amplitude nonreciprocity Δ , while the phase difference of coupling coefficients $\vartheta_1 - \vartheta_2$ influences them weakly. In this connection, for simplicity we consider the coupling coefficients below as complex-conjugate ones ($\vartheta_1 - \vartheta_2 = 0$).

3. Experimental setup

Experiments were performed by using a Nd : YAG diode-pumped monoblock SRL [1]. The chip laser under study was a monoblock with a spherical input face and three total internal reflection faces. The geometrical perimeter of the resonator was 2.6 cm and the resonator nonplanarity angle was 80°. The laser was pumped by a 250-mW, 0.81- μ m diode laser. The white-noise generator in the power circuit of the diode emitter was used for the additional noise pump modulation. The laser under study operated in a single-mode regime (the fundamental mode with one and the same longitudinal index was excited in each direction), which was controlled by the Fabry–Perot interferometer. During the research, the temporal dependences of intensities and radiation power spectra of counterpropagating waves were measured for different pump noise levels. The laser operated in the self-modulation regime of the first kind. When the pump level was changed, the self-modulation period-doubling bifurcation appeared.

4. Experimental results

We studied the evolution of self-modulation oscillations by smoothly changing the control parameter. This control parameter was the excess of the pump power over the lasing threshold η . Both experimental studies and numerical simulations were performed.

The value of η was changed in the range from 0.05 to 0.5 in the experiments. The research performed showed that in a broad value range of η (except the interval $0.22 < \eta < 0.37$) the laser exhibited the self-modulation regime of the first kind. In the interval $0.22 < \eta < 0.37$ the period-doubling regime of self-modulation oscillations appeared.

4.1 Temporal and spectral emission parameters

Figure 1 presents the experimental dependences of the self-modulation frequency ω_m and doubled relaxation frequency $2\omega_r$ on η as well as the dependence of ω_m on η obtained in

the numerical simulation. When η increases, the frequency ω_r of relaxation oscillations increases and the self-modulation frequency ω_m changes insignificantly. As a result, for $\omega_r \sim \omega_m/2$ the parametric frequency synchronisation of self-modulation and relaxation oscillations ($\omega_r = \omega_m/2$) appears, which is accompanied by the excitation of relaxation oscillations and by the period doubling of the radiation self-modulation. The regime with the doubled period of oscillations exists in the finite interval of changes in the control parameter $\eta_1 < \eta < \eta_2$, where $\eta_{1,2}$ are the left and right boundaries of the parametric synchronisation region.

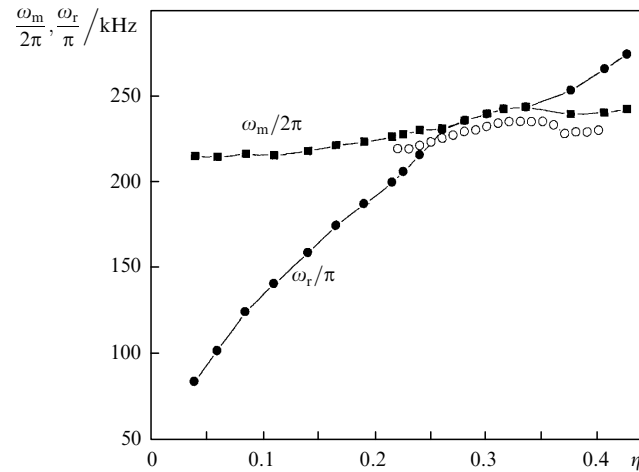


Figure 1. Dependences of the self-modulation frequency $\omega_m/2\pi$ and doubled relaxation frequency ω_r/π on the pump excess over the threshold (■, ● are the results of the experiment, ○ is the numerical simulation).

In the period-doubling regime, the radiation self-modulation of intensities of counterpropagating waves becomes nonsinusoidal and each its period has two intensity maxima. The bifurcation diagrams in Fig. 2 show the change in the intensity maxima of counterpropagating waves by varying η . According to the presented diagrams when η is increased, the difference between two adjacent intensity maxima proves to be significant first only in one beam while in the other (counterpropagating) the adjacent maxima almost coincide. The difference between the maxima in the first beam increases with increasing η and at $\eta = 0.3$ becomes the largest. When η is further increased, similar changes take place in the counterpropagating beam, while in the first one, on the contrary, the adjacent maxima become almost the same. The experimental diagrams are analogous to those obtained in the numerical simulation.

The asymmetry for counterpropagating laser waves is observed not only in bifurcation diagrams but also in the difference in the character of the radiation self-modulation of counterpropagating waves. Figure 3 shows the time dependences of intensities of counterpropagating waves inside the period-doubling region for three values of the control parameter η . These dependences were measured experimentally. The dependences obtained in the numerical simulation are completely similar to those presented in Fig. 3. Inside the period-doubling region the radiation power spectra also can differ significantly for counterpropagating directions, which is seen in Fig. 4.

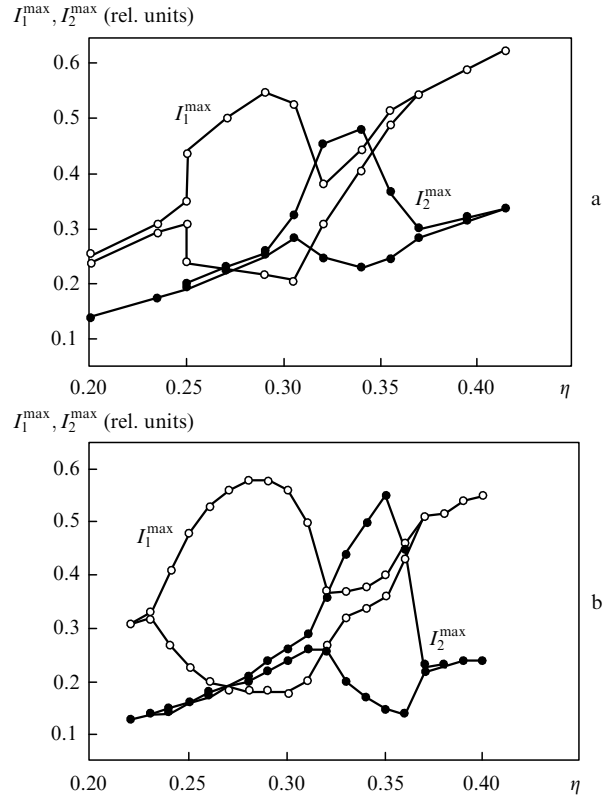


Figure 2. Bifurcation diagrams showing the change in the intensity maxima of counterpropagating waves by varying η (a is the experiment, b is the numerical simulation).

The difference in the temporal and spectral emission parameters for counterpropagating directions can appear in the model under study both due to the inequality of the moduli of the feedback coefficient $m_{1,2}$ and due to the amplitude nonreciprocity of the ring resonator $\Delta = \omega_c/Q_2 - \omega_c/Q_1$. In the self-modulation regime of the first kind the amplitude nonreciprocity can be experimentally measured by the phase shift $\delta\varphi$ of the self-modulation signals in counterpropagating waves. In the absence of

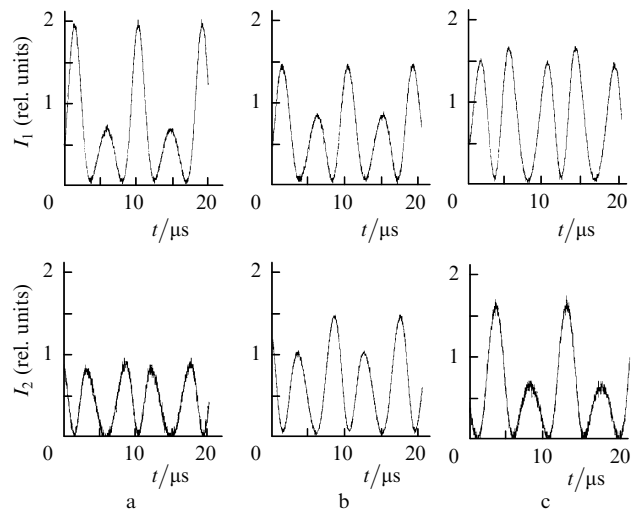


Figure 3. Time dependences of the intensities of counterpropagating waves inside the period-doubling region for $\eta = 0.275$ (a), 0.3 (b) and 0.34 (c).

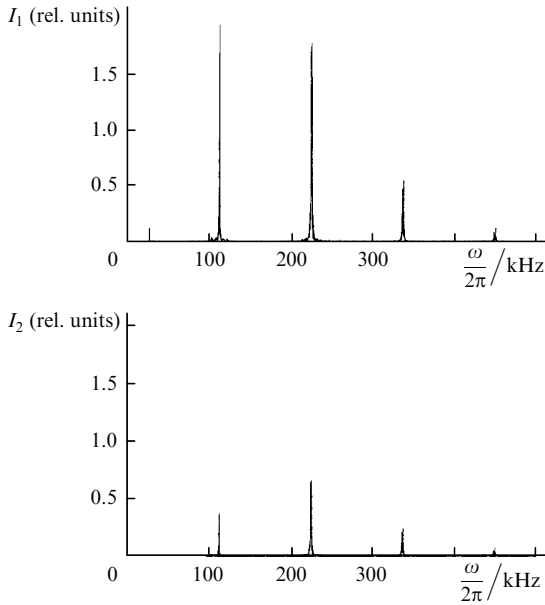


Figure 4. Radiation power spectra for counterpropagating waves for $\eta = 0.275$.

the amplitude nonreciprocity ($\Delta = 0$), the intensity self-modulation of counterpropagating waves is strictly out-of-phase. If $\Delta \neq 0$, the out-of-phase propagation is violated, which is characterised by the phase shift

$$\sin \delta\varphi = 2\Delta/\omega_m. \tag{7}$$

The experimental dependence of $\delta\varphi$ on the pump excess over the threshold is shown in Fig. 5. The same figure presents the values of Δ calculated by using expression (7). It was assumed in the numerical simulation that $\Delta = 5000 \text{ s}^{-1}$. To obtain a satisfactory agreement with the results of the experiment we used the following values of the moduli of coupling coefficients: $m_1 = 812600 \text{ s}^{-1}$, $m_2 = 1986400 \text{ s}^{-1}$.

We measured the peak width $\delta\nu_m$ at the frequency of the self-modulation oscillations in the radiation power spectrum. Our measurements showed that in the self-modulation regime of the first kind, $\delta\nu_m$ is almost independent of the pump excess over the threshold and is equal to $\sim 4 \text{ kHz}$. The parametric synchronisation of the frequencies of self-modulation and relaxation oscillations caused a decrease in

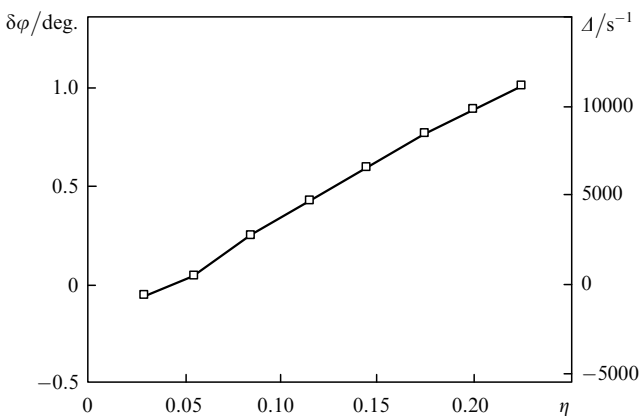


Figure 5. Experimental dependence of $\delta\varphi$ on the pump excess over the threshold and the value Δ calculated by using expression (7).

the peak widths at frequencies ω_m and ω_r . In the period-doubling region of self-modulation (for $0.22 < \eta < 0.37$) the width decreased approximately twice.

4.2 Noise precursors of the period-doubling bifurcation of the self-modulation

We observed the noise precursors (two closely spaced peaks at the frequency ω_r and combination frequency $\omega_m - \omega_r$) near the bifurcation point in the radiation power spectrum. In Fig. 6 these precursors are shown when η increases till the appearance of the bifurcation. One can see that as the bifurcation point is approached the precursors become closer to each other and increase in their intensity. The noise precursors presented in Fig. 6 appear under the action of intrinsic noises of the system. In this paper we also studied the influence of the additional pump noise on the precursor characteristics of the period-doubling bifurcation. It was shown that the noise pump modulation affects the position (central frequency) of precursor peaks and their width.

Figure 7 shows the dependences of the central peaks of precursors on the noise intensity near the period-doubling bifurcation point obtained in the experiment and numerical

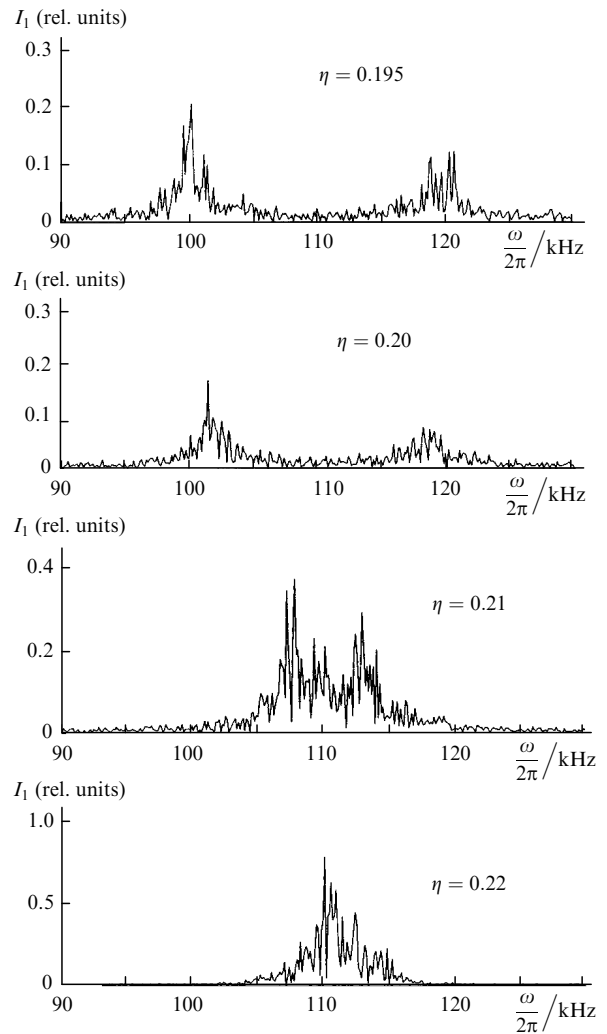


Figure 6. Noise precursors of the period-doubling bifurcation in the radiation power spectrum with increasing η up to the bifurcation appearance.

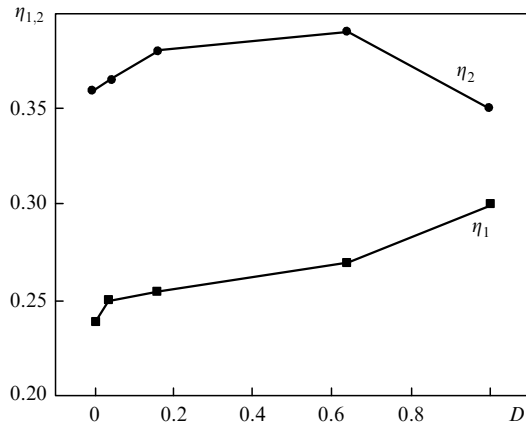


Figure 8. Experimentally measured boundaries of the doubling region $\eta_{1,2}$ as a function of the noise intensity D .

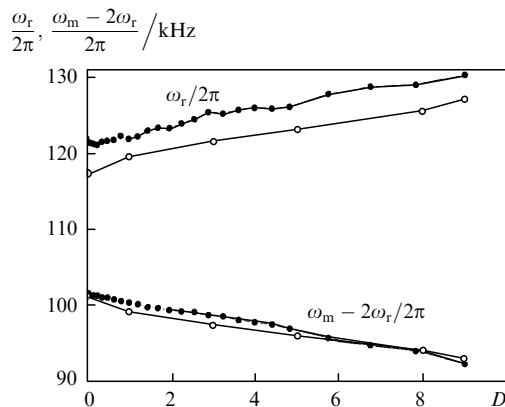


Figure 7. Dependences of the central frequencies of noise precursor peaks on the relative noise intensity D near the period-doubling bifurcation point (● are the results of the experiment, ○ is the numerical simulation).

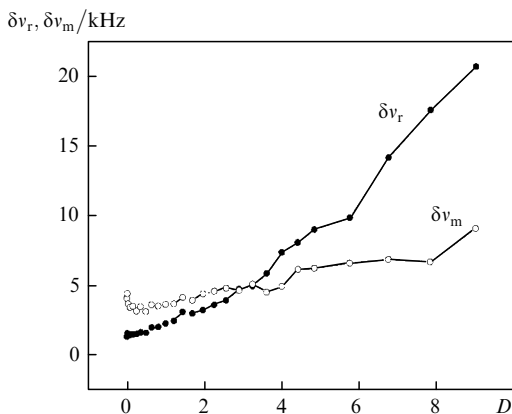


Figure 9. Dependence of the noise modulation of the pump on the peak widths of self-modulation (δv_m) and relaxation (δv_r) oscillations near the bifurcation point (experiment).

simulation. One can see that when the noise increases, the precursors ‘push apart’ nonlinearly due to which the boundaries of the period-doubling region are displaced resulting in the increase in η . Figure 8 presents the experimentally measured boundaries of the doubling region $\eta_{1,2}$ as a function on the noise intensity.

The influence of the noise modulation of the pump on the peak widths of modulation and relaxation oscillations was studied near the bifurcation point (Fig. 9). One can see that the line width at the frequency of self-modulation oscillations weakly depends on the pump noise intensity and the peak width at the fundamental relaxation frequency significantly increases (approximately by an order of magnitude) with its increase.

5. Conclusions

We have studied in this paper the characteristics of self-modulation oscillations when period-doubling bifurcation appears. It has been shown that the inequality of the coupling coefficients of counterpropagating waves and the amplitude nonreciprocity of the ring resonator lead to the difference of temporal and spectral emission parameters of counterpropagating waves. The dependence of the line width at the self-modulation frequency on the pump excess over the threshold has been studied. It has been shown that when the period is doubled, the width of the spectral peak at the self-modulation frequency decreases by twice. The influence of the pump noise on the precursors of the period-doubling bifurcation has been studied. Due to the shift of the noise precursor frequencies, the bifurcation point is displaced under the noise action.

Acknowledgements. This work was supported by Russian Foundation for Basic Research (Grant Nos 07-02-00204 and 08-02-00217).

References

1. Kravtsov N.V., Lariontsev E.G. *Kvantovaya Elektron.*, **36**, 192 (2006) [*Quantum Electron.*, **36**, 192 (2006)].
2. Kravtsov N.V., Lariontsev E.G. *Kvantovaya Elektron.*, **34**, 487 (2004) [*Quantum Electron.*, **34**, 487 (2004)].
3. Zolotoverkh I.I., Lariontsev E.G. *Kvantovaya Elektron.*, **22**, 1171 (1995) [*Quantum Electron.*, **25**, 1131 (1995)].
4. Zolotoverkh I.I., Kravtsov N.V., Lariontsev E.G., Makarov A.A., Firsov V.V. *Kvantovaya Elektron.*, **22**, 213 (1995) [*Quantum Electron.*, **25**, 197 (1995)].
5. Kravtsov N.V., Lariontsev E.G. *Laser Phys.*, **7**, 196 (1997).
6. Zolotoverkh I.I., Kravtsov N.V., Kravtsov N.N., Lariontsev E.G., Makarov A.A. *Kvantovaya Elektron.*, **24**, 638 (1997) [*Quantum Electron.*, **27**, 621 (1997)].
7. Wiesenfeld K., McNamara B. *Phys. Rev. Lett.*, **55**, 13 (1985); *Phys. Rev. A*, **33**, 629 (1986).
8. Wiesenfeld K. *Phys. Rev. A*, **33**, 4026 (1986).
9. Bryant P., Wiesenfeld K. *Phys. Rev. A*, **33**, 2525 (1986).
10. Eckmann J.P. *Rev. Mod. Phys.*, **53**, 643 (1981).
11. Kravtsov Yu.A., Bil'chinskaya S.G., Butkovskii O.Ya., Rychka I.A., Surovyatkina E.D. *Zh. Eksp. Teor. Fiz.*, **12**, 1527 (2001).
12. Kravtsov Yu.A., Surovyatkina E.D. *Phys. Lett. A*, **319**, 348 (2003).
13. Glorieux P., Lepers C., Corbalan R., Cortit J., Pisarchik A.N. *Opt. Commun.*, **118**, 309 (1995).
14. Corbalan R., Cortit J., Pisarchik A.N., Chizhevsky V.N., Vilaseca R. *Phys. Rev. A*, **51**, 663 (1995).
15. Wiesenfeld K. *Phys. Rev. A*, **32**, 1744 (1986).
16. Lamela H., Perez S., Carpintero G. *Opt. Lett.*, **26**, 69 (2001).
17. Neiman A., Saporin P.I., Stone L. *Phys. Rev. E*, **56**, 270 (1997).
18. Kiss I.Z., Hudson J.L., Escalera Santos G.J., Parmananda P. *Phys. Rev. E*, **67**, 035201 (2003).
19. Zolotoverkh I.I., Kravtsov N.V., Lariontsev E.G., Firsov V.V., Chekina S.N. *Kvantovaya Elektron.*, **37**, 1011 (2007) [*Quantum Electron.*, **37**, 1011 (2007)].